

See discussions, stats, and author profiles for this publication at: <https://www.researchgate.net/publication/278412069>

Direct and Dry Deposited Single-Walled Carbon Nanotube Films Doped with MoO_x as Electron-Blocking Transparent Electrodes for Flexible Organic Solar Cells

ARTICLE in JOURNAL OF THE AMERICAN CHEMICAL SOCIETY · JUNE 2015

Impact Factor: 12.11 · DOI: 10.1021/jacs.5b03739

CITATIONS

2

READS

86

8 AUTHORS, INCLUDING:



Il Jeon

The University of Tokyo

15 PUBLICATIONS 16 CITATIONS

SEE PROFILE



Anton S. Anisimov

Canatu Inc.

21 PUBLICATIONS 481 CITATIONS

SEE PROFILE



Albert G Nasibulin

Skolkovo Institute of Science and Technology

231 PUBLICATIONS 3,828 CITATIONS

SEE PROFILE



Shigeo Maruyama

The University of Tokyo

406 PUBLICATIONS 8,028 CITATIONS

SEE PROFILE

Direct and Dry Deposited Single-Walled Carbon Nanotube Films Doped with MoO_x as Electron-Blocking Transparent Electrodes for Flexible Organic Solar Cells

Il Jeon,[†] Kehang Cui,[‡] Takaaki Chiba,[‡] Anton Anisimov,[§] Albert G. Nasibulin,^{#,¶} Esko I. Kauppinen,[#] Shigeo Maruyama,^{*,‡} Yutaka Matsuo^{*,†}

[†] Department of Chemistry, School of Science, The University of Tokyo, 7-3-1 Hongo, Bunkyo-ku, Tokyo 113-0033, Japan

[‡] Department of Mechanical Engineering, School of Engineering, The University of Tokyo, 7-3-1 Hongo, Bunkyo-ku, Tokyo 113-8656, Japan

[§] Canatu Ltd., Konalankuja 5, FI-00390 Helsinki, Finland

[#] Department of Applied Physics, Aalto University School of Science, 15100, FI-00076 Aalto, Finland

[¶] Skolkovo Institute of Science and Technology, 100 Novaya str., Skolkovo, Moscow Region, 143025, Russia

Supporting Information Placeholder

ABSTRACT: Organic solar cells have been regarded as a promising electrical energy source. Transparent and conductive carbon nanotube film offers an alternative to commonly used ITO in photovoltaics with superior flexibility. This paper reports carbon nanotube based indium-free organic solar cells and their flexible application. Direct- and dry-deposited carbon nanotube film doped with MoO_x functions as an electron-blocking transparent electrode and its performance is enhanced further by over-coating PEDOT:PSS. Single-walled carbon nanotube organic solar cell in this work shows the power conversion efficiency of 6.04%. This value is 83% of the leading ITO-based device performance (7.48%). Flexible application shows 3.91% efficiency and is capable of withstanding a severe cyclic flex test.

Carbon nanotubes (CNT) and graphene have emerged as materials for next-generation electrodes in organic solar cells (OSCs), offering a possible alternative to indium tin oxide (ITO)-based OSCs.¹ CNTs and graphene have excellent mechanical flexibility and are composed entirely of highly abundant carbon. Single-walled CNTs (SWCNTs) have advantages in terms of stretchability,² ease of synthesis, and suitability for direct roll-to-roll deposition onto substrates, which translate into lower costs. SWCNTs as transparent conductive films in photovoltaics have been the subject of active research.³

For the researches in OSCs are concerned, they have attracted a great deal of attention as solution-processable and flexible light-harvesting devices that have the potential to meet the world's energy needs. The efficiency of OSCs has increased tremendously with the development of low band gap polymers⁴ which enabled absorption of longer wavelengths of the solar spectrum and, thus led to larger short-circuit current (J_{sc}). As the result, power conversion efficiency (PCE) has reached as high as 10%. However, OSC flexibility⁵ is still

limited by the use of ITO, which is bendable but not completely flexible nor stretchable like CNTs.

The objective of this study was to develop the best methodology for ITO-free SWCNT-utilized efficient OSC fabrication. First, a free-standing CNT electrode was prepared by direct- and dry-deposition of SWCNTs grown by an aerosol chemical vapor deposition technique.⁶ Compared with other solution-based processes,⁷ our process uses no surfactant and induces less defects. Moreover, electrical performance of the films produced by this method was higher than that of other CNT films including flexible ITO. Second, MoO₃ doping, which was originally proposed by Bao *et al.*,⁸ was employed and optimized for other reported dopants are unstable to air, chemicals, thermal stress, and humidity.^{3a} Thirdly, for the photoactive layer is concerned, the low band gap polymer, thieno[3,4-*b*] thiophene/benzodithiophene (PTB7)⁹ was used for its high performance among organic photoactive materials. In addition, PTB7's does not require thermal annealing. This enabled us the use of flexible substrates.¹⁰

The present SWCNT OSCs showed a PCE of 6.04% with the PTB7:PC₇₁BM photoactive layer. In addition, flexible OSCs on polyimide (PI) and polyethylene terephthalate (PET) films gave PCEs of 3.43% and 3.91%, respectively. We anticipate that the methodology presented here will help pave the way towards carbon-based flexible solar cells.

We first investigated thickness dependence of the SWCNT films on photovoltaic property of SWCNT-OSCs by varying the deposition time of the SWCNT production. We obtained three thicknesses that gave 65%, 80%, and 90% transparency at 550 nm.¹¹ The atomic force (AFM) microscopy showed that all the SWCNT films have similar root mean square roughness of 8 to 10 nm (Fig. S2). For the device fabrication, we used poly(3-hexylthiophene) (P3HT) as a donor, because it is a benchmark material in the field of OSCs, and most CNT OSCs reported to date have also used this material.^{3a} Therefore, valid comparisons could be made. Using this material, OSCs were fabricated on SWCNT films with different thicknesses (transparency). Fast growth method¹² was adopted for high perfor-

mance without solvent annealing. MoO₃ was used here as an electron-blocking layer and it was not subjected to thermal annealing. Three devices with various thicknesses of SWCNT films showed similar PCEs of under 1% (Table S1). The similarity of the PCEs is due to the trade-off between J_{SC} and fill factor (FF), which are closely related to the transparency and the conductivity, respectively. The overall performances were poor and doping was called for.

MoO₃ was subjected to thermal annealing on SWCNT for the doping. In previous work, bottom MoO₃ under spray-coated CNTs was thermally annealed at 450–500 °C for more than 3 h in Ar.⁸ However, in this work, we annealed MoO₃ on top of the aerosol SWCNT films at 300 °C for 3 h in N₂, considering the use of flexible PI substrates which has glass transition temperature (T_g) of 320 °C. Utilizing this thermally-driven hole doping from MoO₃ to SWCNT, device gave a PCE of 1.91% which is nearly twice the improvement from the non-annealed device (Table S3, devices A and B; Fig. 2a). Corresponding $J-V$ curves are shown in Figure S3. Both increase in J_{SC} and decrease in R_s were observed, and these are indications of improved transmittance and conductivity of the SWCNTs. High shunt resistance (R_{SH}) even after the thermal annealing indicates that thermally annealed MoO₃ can still function as an electron-blocking layer.

We further investigated the doping effect. The doping was visually confirmed by MoO₃ color change from transparent green to deep blue (Fig. S4). It is caused by oxygen deficiency which induces electron traps that increase absorbance in the deep-blue wavelengths region.¹³ MoO₃ is changed to MoO_x, where x is less than 3. UV-vis spectra show MoO₃-thermally doped SWCNT films having higher transmittance compared with the pristine SWCNT films (Fig. 1a and b). Furthermore, thin 90%- and 80%-SWCNT films displayed the absorption curve with higher transparency at 400–500 nm but less transparency at long-wavelength region due to the absorption by MoO_x (Fig. 1b, Fig. S4). Thus, we hypothesize that P3HT, which absorbs shorter wavelengths of light, is compatible with the 90% transparent SWCNT electrode while PTB7, which absorbs longer wavelengths of light, is more compatible with the 65% transparent SWCNT electrode.

Doping effect was further confirmed by absorption spectra of SWCNT films on quartz substrates (Fig. 1c). Clear peaks for transitions of E₁₁, E₂₂, and M₁₁ in SWCNT indicate the high

quality of aerosol CVD synthesis. Those peaks were suppressed a little when MoO₃ was deposited on SWCNT, and almost completely when it is followed by 2 h of thermal annealing as an indication of successful doping. In addition, decrease in resistivity of the SWCNT films after thermal doping provided further evidence of the doping (Table S2).

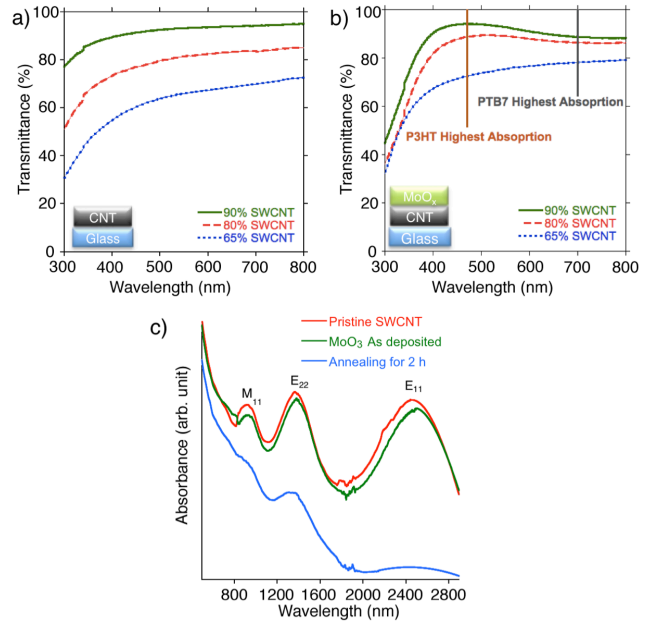


Figure 1. Optical property of SWCNT films with different thicknesses. (a) UV-vis transmittance for pristine SWCNTs films. (b) UV-vis transmittance for SWCNT films after depositing MoO₃ and thermally annealing at 300 °C for 2 h in N₂ with indications of the highest absorption wavelength of P3HT and PTB7. (c) Absorbance in infrared region for SWCNT film pristine (red), with MoO₃ on top (green), and after annealing for 2 h (blue).

Work functions were measured by photoelectron yield spectroscopy. We found that the thermal doping narrowed the gap between the Fermi levels of SWCNT and MoO₃. Pristine SWCNT films on glass exhibited a work function of 4.86 eV. After the thermal annealing with MoO₃, its work function increased to 5.4 eV (Fig. 2c). The work function of MoO₃ is reported to be 6.75 eV¹⁴ and the annealing decreased its work

Table 1. Photovoltaic performance for the optimized SWCNT-MoO_x OSCs.^a

Substrate	Anode	Donor	V_{oc} (V)	J_{sc} (mAcm ⁻²)	FF	R_s (Ωcm ²)	R_{SH} (Ωcm ²)	PCE _{best} (%)
Glass	ITO/MoO ₃	P3HT	0.60	9.42	0.50	23.5	1.56 × 10 ⁴	2.83
Glass	MoO _x /90%-SWCNT/MoO _x /PEDOT:PSS		0.59	8.84	0.46	116	7.05 × 10 ³	2.43
Glass	ITO/MoO ₃	PTB7	0.74	15.5	0.64	31.1	1.18 × 10 ⁷	7.31
Glass	MoO _x /65%-SWCNT/MoO _x /PEDOT:PSS		0.72	13.7	0.61	51.6	1.22 × 10 ⁴	6.04
PI	MoO _x /65%-SWCNT/MoO _x /PEDOT:PSS		0.69	11.3	0.44	454	1.15 × 10 ⁵	3.43
PI	After 10-time cyclic flex test		0.70	11.1	0.27	588	3.85 × 10 ⁴	2.10
Glass	65%-SWCNT/MoO ₃ /PEDOT:PSS	PTB7	0.70	12.7	0.58	94.5	4.00 × 10 ⁴	5.27
PET	65%-SWCNT/MoO ₃ /PEDOT:PSS		0.69	12.6	0.45	160	2.06 × 10 ³	3.91
PET	After 10-time cyclic flex test		0.69	12.3	0.45	222	2.83 × 10 ³	3.82

^a MoO₃ and MoO_x represent as-deposited MoO₃ and thermal annealed, respectively. 90%-, 80%-, and 65%-SWCNT denotes 90%, 80%, and 65% transparent SWCNT films.

function to 6.00 eV.

The PCE of doped SWCNT-based device was still lower than the ITO based device. Thus, we analyzed the morphology of the MoO_x on SWCNT. The scanning electron microscopy (SEM) images indicated that there are pinholes created on MoO_x film after the annealing (Fig. S5d and e); the AFM r.m.s. roughness value of 9.7 increased to 23.1 (Fig. S5a and b). To find a solution to this, we tested various configurations involving additional MoO_3 and PEDOT:PSS. Use of extra MoO_3 on MoO_x decreased J_{SC} (Table S3, devices C and D), which is attributable to mismatching in energy levels. Whereas when PEDOT:PSS was over-coated on MoO_x , both V_{OC} and J_{SC} were enhanced (Table S3, device E; Fig. S6). We ascribe this to the hydrophilic nature of hydroxyl groups on MoO_x and solution coating method which allows PEDOT:PSS to fill up the pinholes more effectively. Besides, the acidic PEDOT:PSS can also function as a weak additional dopant (Fig. S5c and f).¹⁵ With the optimized configuration, a PCE of 2.34% was achieved (Table S3, device G; Fig. 2b). Moreover, applying sandwich doping of MoO_x above and below SWCNT film enhanced the performance even further, giving a PCE of 2.43% (Table 1). This value is 86% of the corresponding ITO-based OSC's efficiency (2.83%; Table 1; Fig. 3a).

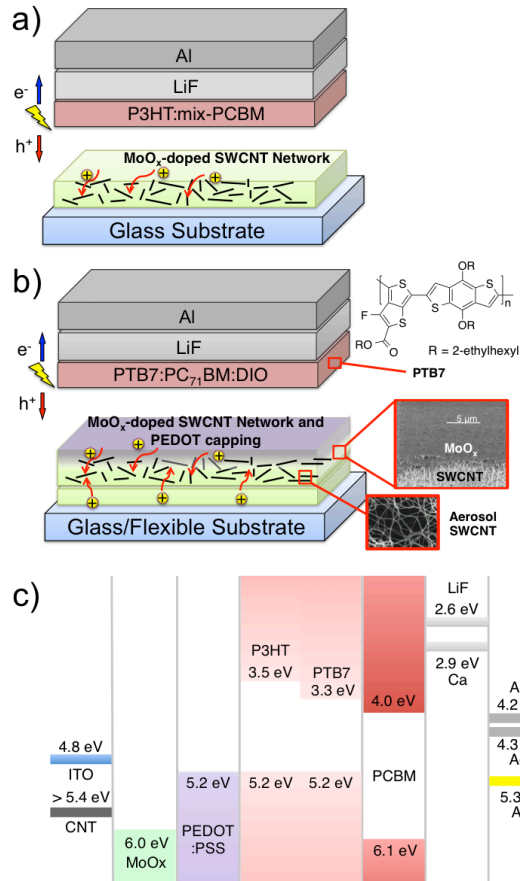


Figure 2. SWCNT OSCs configurations of (a) P3HT-based cells (glass/SWCNT/ MoO_x /P3HT:mix-PCBM/LiF/Al) and (b) the most optimized device that gave high efficiency (glass or flexible substrate/ MoO_x /SWCNT/ MoO_x /PEDOT:PSS/PTB7:PC₇₁BM/LiF/Al) (c) Energy band alignment diagram of SWCNT OSCs.

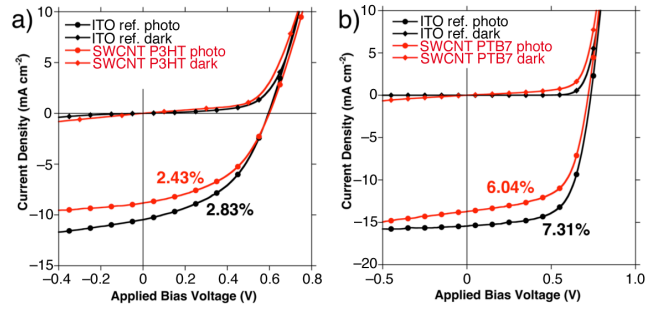


Figure 3. J - V Curves of the two optimized SWCNT OSCs (red lines) in comparison with reference ITO-based OSCs under light and dark conditions. (a) P3HT:mix-PBM-based devices (b) PTB7:PC₇₁BM-based devices.

Another unique phenomenon of SWCNT-based OSCs is that it was not compatible with Ca/Al cathode unlike its ITO counterpart (Table S4).¹⁶ This is because Ca causes non-spontaneous electron extraction as Eo and his colleagues have demonstrated.¹⁷ Although LiF possesses the work function of 2.6 eV, which seems not compatible with the energy levels of Al and PCBM, it is extremely thin (0.7 nm). Thus, it can act as a protective layer only without interfering energetically.

Next, we tested the low band gap polymer, PTB7 for the first time in CNT OSCs. The OSC device with the 65% transparent SWCNT film gave a PCE of 6.04%, which is record-high result (Fig. 2b; Fig. 3b; Table 1; see also Fig. 4 and Fig. S9). This is 83% of the ITO-based device efficiency (7.48%; Table 1). This result reveals that the low band gap polymer system is also compatible with existing SWCNT-based electrodes.

Finally, flexible application was accomplished using both PI and PET as substrates. PI's high T_g enabled thermal annealing of MoO_3 , but PET with T_g of 80 °C could not be annealed. Initially, the flexible OSCs gave PCEs of 3.78% (PI) and 3.91% (PET) (Table 1). We ascribe the low performance in both the flexible devices to the damage on MoO_3 during fabrication by looking at the decrease in R_s . Additionally, the PI device's low J_{SC} was limited by the intrinsically low transparency of the film (Fig. S7). The PET-based device to which thermal annealing was not applied gave a higher PCE than that of the PI-based device. After subjecting the devices to 10 flexing cycles (radius of curvature: 5 mm), the PET-based flexible OSC retained its performance, while the PI-based flexible OSC significantly decreased the performance (Fig. S8; Table 1). This points towards the fact that PI based device is strongly affected by the high temperature annealing.

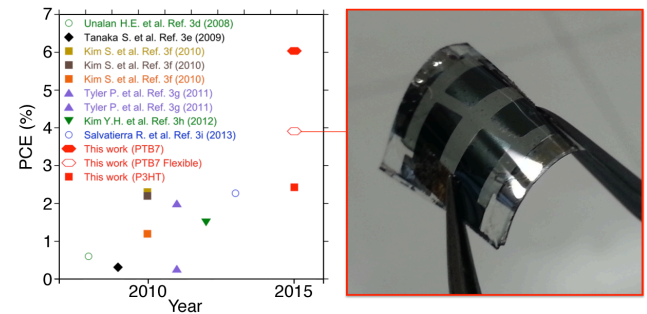


Figure 4. Reported PCEs of CNT OSCs on glass (closed symbols) and on flexible substrate (open symbols) (left) and a picture of the present PET-based flexible SWCNT OSC (right).

In summary, this work showed a way for efficient and flexible CNT-based OSCs with application of direct- and dry-deposited SWCNT film in OSCs, and demonstrated the dual functionality of thermally annealed MoO_x on SWCNTs as both transparent electrode and electron-blocking layer. Thus, the MoO_x/SWCNT worked as an electron-blocking transparent electrode. The PTB7 system was applied in CNT OSCs and produced a high PCE as well as successfully exhibiting flexible application. Taken together, our findings demonstrate that ITO-free flexible SWCNT OSCs can be fabricated with high efficiency through a remarkably facile and stable process. We anticipate that these results will be useful in the further development of flexible carbon-based solar cells as well as other related organic electronics.

ASSOCIATED CONTENT

Supporting Information. Experimental pictures, AFM and SEM images, UV-vis spectra, data for conductivity measurements, *J*-*V* curves, IPCE, statistical analysis. This material is available free of charge via the Internet at <http://pubs.acs.org>.

AUTHOR INFORMATION

Corresponding Author

maruyama@photon.t.u-tokyo.ac.jp

matsuo@chem.s.u-tokyo.ac.jp

Notes

The authors declare no competing financial interest.

ACKNOWLEDGMENT

This work was partly supported by Grants-in-Aid for Scientific Research (22226006, 25107002, 15H02219), IRENA project by JST-EC DG RTD, Strategic International Collaborative Research Program, SICORP (S.M. and Y.M.), MOPPI and Ministry of Education and Science of Russian Federation (Project DOI: RFMEFI58114X0006) (A.N. and E.K.). The authors also thank the Funding Program for Next-Generation World-Leading Researchers (Y.M.), the JSPS Grand-in-Aid for Young Scientists (15K17983) (K.C.), and Japan Student Services Organization (I.J.).

REFERENCES

- (1) De Volder, M. F. L.; Tawfick, S. H.; Baughman, R. H.; Hart, A. J. *Science* **2013**, 339, 535.
- (2) Won, S.; Hwangbo, Y.; Lee, S.-K.; Kim, K.-S.; Kim, K.-S.; Lee, S.-M.; Lee, H.-J.; Ahn, J.-H.; Kim, J.-H.; Lee, S.-B. *Nanoscale* **2014**, 6, 6057.
- (3) a) Du, J.; Pei, S.; Ma, L.; Cheng, H.-M. *Adv. Mater.* **2014**, 26, 1958. b) Park, H.-S.; Chang, S.; Zhou, X.; Kong, J.; Palacios, T.; Gradecak, S. *Nano Lett.* **2014**, 14, 5148. c) Zhen, L.; Kulkarni, S. A.; Boix, P. P.; Shi, E.; Cao, A.; Fu, K.; Batabyal, S. K.; Zhang, J.; Xiong, Q.; Wong, L. H.; Mathews, N.; Mhaisalkar, S. G. *ACS Nano* **2014**, 8, 6797. d) Unalan, H. E.; Hiralal, P.; Kuo, D.; Parekh, B.; Amaratunga, G.; Chhowalla, M. *J. Mater. Chem.* **2008**, 18, 5909. e) Tanaka, S.; Mielczarek, K.; Ovalle-Robles, R.; Wang, B.; Hsu, D.; Zakhidov, A. A. *Appl. Phys. Lett.* **2009**, 94, 113506. f) Kim, S.; Yim, J.; Wang, X.; Bradley, D. D. C.; Lee, S.; deMello, J. C. *Adv. Funct. Mater.* **2010**, 20, 2310. g) Tyler, T. P.; Brock, R. E.; Karmel, H. J.; Marks, T. J. and Hersam, M. C. *Adv. Energy Mater.* **2011**, 1, 785. h)

- Kim, Y. H.; Müller-Meskamp, L.; Zakhidov, A. A.; Sachse, C.; Meiss, J.; Bikova, J.; Cook, A.; Zakhidov, A. A.; Leo, K. *Sol. Energy Mater. Sol. Cells* **2012**, 96, 244. i) Salvatierra, R. V.; Cava, C. E.; Roman, L. S.; Zharbin, A. J. G. *Adv. Funct. Mater.* **2013**, 23, 1490. j) Cui, K.; Anisimov, A. S.; Chiba, T.; Fujii, S.; Kataura, H.; Nasibulin, A. G.; Chiashi, S.; Kauppinen, E. I.; Maruyama, S. *J. Mater. Chem. A* **2014**, 2, 11311. k) Dabera, G. D. M. R.; Jayawardena, K. D. G. I.; Prabhath, M. R. R.; Yahya, I.; Tan, Y. Y.; Nismy, N. A.; Shiozawa, H.; Sauer, Markus.; Ruiz-Soria, G.; Ayala, P.; Stolojan, V.; Adikaari, A. A. D. T.; Jarowski, P. D.; Pichler, T.; Silva, S. R. P. *ACS Nano* **2013**, 7, 556. l) Maiti, U. N.; Lee, W. J.; Lee, J. M.; Oh, Y.; Kim, J. Y.; Kim, J. E.; Shim, J.; Han, T. H.; Kim, S. O. *Adv. Mater.* **2014**, 26, 40. m) Lee, J. M.; Kwon, B.; Park, H. I.; Kim, H.; Kim, H. G.; Park, J. S.; Kim, E. S.; Yoo, S.; Jeon, D. Y.; Kim, S. O. *Adv. Mater.* **2013**, 25, 2011. n) Li, D. J.; Maiti, U. N.; Lim, J.; Choi, D. S.; Lee, W. J.; Oh, Y.; Lee, G. Y.; Kim, S. O. *Nano Lett.* **2014**, 14, 1228. o) Park, J. S.; Lee, J. M.; Hwang, S. K.; Lee, S. H.; Lee, H.-J.; Lee, B. R.; Park, H. I.; Kim, J.-S.; Yoo, S.; Song, M. H.; Kim, S. O. *J. Mater. Chem.* **2012**, 22, 12695. p) Lee, J. M.; Kwon, B.-H.; Park, H. I.; Kim, H.; Kim, M. G.; Park, J. S.; Kim, E. S.; Yoo, S.; Jeon, D. Y.; Kim, S. O. *Adv. Mater.* **2013**, 25, 2011. q) Lee, J. M.; Lim, J.; Lee, N.; Park, H. I.; Lee, K. E.; Jeon, T.; Nam, S. A.; Kim, J.; Shin, J.; Kim, S. O. *Adv. Mater.* **2014**, 27, 2015.
- (4) Blouin, N. and Michaud, A.; Leclerc, M. *Adv. Mater.* **2007**, 19, 2295.
- (5) Kaltbrunner, M.; White, M. S.; Głowacki, E. D.; Sekitani, T.; Someya, T.; Sariciftci, N. S.; Bauer, S. *Nat. Commun.* **2012**, 3, 770.
- (6) Nasibulin, A. G.; Kaskela, A.; Mustonen, K.; Anisimov, A. S.; Ruiz, V.; Kivistö, S.; Rackauskas, S.; Timmermans, M. Y.; Pudas, M.; Aitchison, B.; Kauppinen, M.; Brown, D. P.; Okhotnikov, O. G.; Kauppinen, E. I. *ACS Nano* **2011**, 5, 3214.
- (7) a) Zhou, Y.; Hu, L.; Gruner, G. *Appl. Phys. Lett.* **2006**, 88, 123109. b) Lim, C.; Min, D. H.; Lee, S. B. *Appl. Phys. Lett.* **2007**, 91, 243117.
- (8) Hellstrom, S. L.; Vosgueritchian, M.; Stoltenberg, R. M.; Irfan, I.; Hammock, M.; Wang, Y. B.; Jia, C.; Guo, X.; Gao, Y.; Bao, Z. *Nano Lett.* **2012**, 12, 3574.
- (9) Liang, Y.; Xu, Z.; Xia, J.; Tsai, S. T.; Wu, Y.; Li, G.; Ray, C.; Yu, L. *Adv. Mater.* **2010**, 22, E135.
- (10) He, Z.; Zhong, C.; Su, S.; Xu, M.; Wu, H.; Cao, Y. *Nat. Photonics* **2012**, 6, 591.
- (11) a) Nasibulin, A. G.; Ollikainen, A.; Anisimov, A. S.; Brown, D. P.; Pikhitsa, P. V.; Holopainen, S.; Penttilä, J. S.; Helistö, P.; Ruokolainen, J.; Choi, M.; Kauppinen, E. I. *Chem. Eng. J.* **2008**, 136, 409. b) Kaskela, A.; Nasibulin, A. G.; Timmermans, M. Y.; Aitchison, B.; Papadimitratos, A.; Tian, Y.; Zhu, Z.; Jiang, H.; Brown, D. P.; Zakhidov, A.; Kauppinen, E. I. *Nano Lett.* **2010**, 10, 4349.
- (12) Xu, Z.; Chen, L.-M.; Yang, G.; Huang, C.-H.; Hou, J.; Wu, Y.; Li, G.; Hsu, C.-S.; Yang, Y. *Adv. Funct. Mater.* **2009**, 19, 1227.
- (13) Mestl, G.; Ruiz, P.; Delmon, B.; Knözinger, H. *J. Phys. Chem.* **1994**, 98, 11269.
- (14) Irfan, Ding, H.; Gao, Y.; Small, C.; Kim, D. Y.; Subbiah, J.; So, F. *Appl. Phys. Lett.* **2010**, 96, 243307.
- (15) Kymakis, E.; Klapsis, G.; Koudoumas, E.; Stratakis, E.; Korniliotis, N.; Vidakis, N.; Franghiadakis, Y. *Eur. Phys. J. Appl. Phys.* **2006**, 36, 257.
- (16) Kumar, A.; Rosen, N.; Devine, R.; Yang, Y. *Energy Environ. Sci.* **2011**, 4, 4917.
- (17) Eo, Y. S.; Rhee, H. W.; Chin, B. D.; Yu, J. W. *Synth. Met.* **2009**, 159, 1910.

Table of Contents Graphic:

